*Progress In Electromagnetics Research, Vol. 126, 121–138, 2012*

# LUMPED DUAL-FREQUENCY IMPEDANCE TRANSFORMERS FOR FREQUENCY-DEPENDENT COMPLEX LOADS

**Y. Liu[1, 2, *], Y. J. Zhao[1], and Y. G. Zhou[1]**

[1]College of Electronic and Information Engineering, Nanjing University of Aeronautics and Astronautics, Nanjing 210016, China

[2]State Key Laboratory of Millimeter Waves, Southeast University, Nanjing 210096, China

**Abstract**—This paper presents lumped dual-frequency impedance transformers for frequency-dependent complex loads. According to different dual-frequency allocations of a complex load in Smith chart, three types of impedance matching networks are presented respectively. Several kinds of lumped circuit blocks are used as basic elements for constructing these transformers with design formula deduced. Various examples are given for describing the design procedures. Good features such as big frequency ratio and big matching bandwidths are demonstrated. These lumped dual-frequency impedance transformers have advantage of much compacter dimensions compared to distributive solutions.

## 1. INTRODUCTION

Impedance transformers are basic building blocks for microwave components such as power amplifiers, power dividers, antennas. Recently as dual-band microwave components are becoming a trend [1–16], the demand for dual-frequency impedance transformers has been increasing. Dual-frequency impedance matching were firstly realized between real impedances [17, 18]. In [17] two sections of transmission line of same length are cascaded to realize a dual-frequency transformer between real impedance load and real impedance source. L-shaped network containing a transmission line and a shunt stub can also realize the same function [18]. As it is usually demanded to realize

*Received 12 December 2011, Accepted 20 February 2012, Scheduled 10 March 2012*

* Corresponding author: Yun Liu (lycloud1978@163.com).

impedance matching from complex loads (such as the input or output impedance of a power amplifier) to a real-impedance source new techniques are proposed [19–22]. In [19] two unequal transmission line sections are cascaded to realize dual-frequency impedance matching for a frequency-independent complex load. As to frequency-dependent complex loads, a three-section impedance transformer is proposed in [20] to realize dual-frequency impedance matching. As an alternative of [20], two sections of transmission lines and a two-section shunt stub are cascaded to form a dual-frequency impedance transformer at the expense of big dimension [21]. A T-shaped network is also introduced for dual-frequency matching for complex loads [22]. In a more general problem, [23] discusses the situation in which both the source and the load are complex and frequency dependent in impedance, and a circuit containing four sections of transmission lines is adopted. The above distributive impedance transformers are always bulky especially when the operating frequencies are below several GHzs, so some lumped and hybrid types of dual-frequency transformers are also developed for decreasing the dimensions [24, 25]. In [24] single-band impedance transformers which are constructed by transmission lines and lumped tanks are cascaded to form multi-band transformers. A frequency mapping technique is adopted in [25] to synthesis a dual-frequency transformer which is realized with lumped elements, but the technique is only limited to conduct impedance matching between real impedances. In this paper, traditional $L$ type impedance transformers are extended while lumped circuit blocks are used to realize frequency-dependent reactances and admittances. According to the dual-frequency allocation of a complex load in Smith chart, three types of topologies are presented. The new impedance transformers contain limited number of lumped elements and are much compacter than transformers constructed by transmission lines.

## 2. THEORY

### 2.1. Topologies and Matching Processes

Figure 1(a) and Fig. 1(b) are two $L$-network impedance transformers (type I and type II) which were commonly used for single-frequency impedance matching in the past. Type-I $L$-network is suitable for impedance matching of a complex load which is located outside the $1 + jx$ circle (unit resistance circle) while type-II $L$-network is for a complex impedance located outside the $1 + jb$ circle (unit conductance circle).

If the normalized impedances (referring to matched impedance $Z_0$) of a frequency-dependent load at two specified frequencies ($f_1$ and

$f_2$) are: $z_l(f_n) = z_{ln}$ $(n = 1, 2)$, then three cases can be classified: A), $z_{l1}$ and $z_{l2}$ are both located outside the $1 + jx$ circle; B), $z_{l1}$ and $z_{l2}$ are both outside of the $1 + jb$ circle; C), $z_{l1}$ and $z_{l2}$ are located within the $1 + jb$ and the $1 + jx$ circle, respectively. It should be noted that it can be classified into either case A or case B when $z_{l1}$ and $z_{l2}$ are

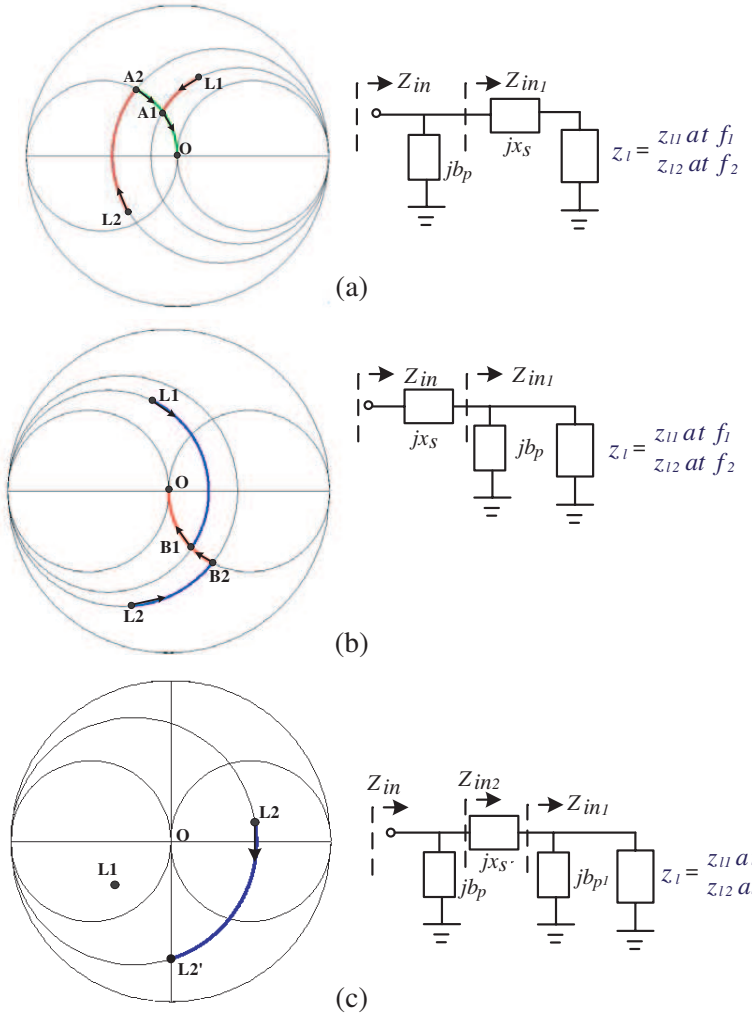


**Figure 1.** Topologies of dual-frequency impedance transformers. (a) $L_1$ and $L_2$ are outside of $1 + jx$ circle. (b) $L_1$ and $L_2$ are outside of $1 + jb$ circle $r$. (c) $L_1$ and $L_2$ are within $1 + jb$ circle and $1 + jx$ circle respectively.

both outside the two circles.

Case A: Each of $z_{l1}$ and $z_{l2}$ can separately get matched via a type-I $L$-Network with certain values of $jb_p$ and $jx_s$, thus they can share one type-I $L$-network provided that the $jb_p$ and $jx_s$ blocks can afford required susceptances and reactances at $f_1$ and $f_2$, respectively. We can see the matching processes in the Smith chart of Fig. 1(a). Here $L_1$ and $L_2$ are the positions of the complex impedances at $f_1$ and $f_2$. By serially connecting the $jx_s$ block, the input impedances at the two frequencies run from $L_1$ and $L_2$ to $A_1$ and $A_2$ via resistance circles. Here $A_1$ and $A_2$ are required to be located on the $1 + jb$ circle. The values of $x_s$ are given as below:

$$x_s(f_n) = \pm\sqrt{r_{ln} - r_{ln}^2} - x_{ln} \qquad n = 1, 2 \tag{1}$$

Here $r_{ln}$ and $x_{ln}$ are the real and imaginary parts of $z_{ln}$. By parallel connecting the shunt admittance of $jb_p$, the impedances run on the $1 + jb$ circle and reach the matching point O respectively. The values of $b_p$ are:

$$b_p(f_n) = \frac{x_s(f_n) + x_{ln}}{r_{ln}^2 + (x_s(f_n) + x_{ln})^2} \qquad n = 1, 2 \tag{2}$$

Case B: If $z_{l1}$ and $z_{l2}$ are both outside of the $1 + jb$ circle, they can share one type-II $L$-network and concurrently get matched if the serial and shunt circuit blocks have needed reactances and suceptances at the two frequencies. As shown in the Smith chart of Fig. 1(b), the input impedances start from $L_1$ and $L_2$ and reach $B_1$ and $B_2$ via conductance circles. Here $B_1$ and $B_2$ are located on the $1 + jx$ circle. This is realized by parallel connecting a $jb_p$ block whose susceptances at the two frequencies are:

$$b_p(f_n) = \pm\sqrt{g_{ln} - g_{ln}^2} - b_{ln} \qquad n = 1, 2 \tag{3}$$

Here $g_{ln}$ and $b_{ln}$ are the real and imaginary parts of the complex admittances of the load. Then by serially connecting a $jx_s$ block, the imaginary part of $z_{in1}$ is compensated at both the two frequencies resulting in matched input impedance $z_{in}$. As a corresponding process in the Smith chart, the impedances go from $B_1$ and $B_2$ and arrive at the matching point O respectively. The formula of the serial reactances are as below:

$$x_s(f_n) = \frac{b_p(f_n) + b_{ln}}{g_{ln}^2 + (b_p(f_n) + b_{ln})^2} \qquad n = 1, 2 \tag{4}$$

Case C: If $z_{l1}$ and $z_{l2}$ are located within $1 + jb$ circle and $1 + jx$ circle respectively, $z_{l1}$ can get matched using a type-II $L$-network and $z_{l2}$ can

be matched by a type-II $L$-network, but they can not share the same $L$-network. For the purpose of dual-frequency impedance matching, the first step is to convert case C to case A or B. As shown in Fig. 1(c), the load is firstly parallel connected with a susceptance $jb_{p1}$ under the constraint condition that $b_{p1}(f_1) = 0$, thus the input impedance at $f_1$ keeps unchanged in the Smith chart while the input impedance at $f_2$ runs on a conductance circle and reaches $L_2'$ which is on the vertical axe (the real part of reflection coefficient is zero), being outside of the $1 + jx$ circle. After this we can follow the same matching procedure as case A. We give the needed susceptance at $f_2$ as:

$$b_{p1}(f_2) = \pm\sqrt{1 - g_{l2}^2} - b_{l2} \tag{5}$$

### 2.2. Lumped Blocks for Dual-frequency Susceptances and Reactances

An important task in realizing the dual-frequency impedance transformers of Fig. 1 is to construct lumped blocks which afford the needed values of susceptances or reactances at two specified frequencies.

To realize various two-frequency susceptances, four types of lumped circuit blocks as shown in Fig. 2 can be adopted. The susceptance of a parallel $LC$ block in Fig. 2(a) is monotone increasing thus suitable for the case that $b_p(f_2)$ is greater than $b_p(f_1)$. Serial $LC$ block as shown in Fig. 2(b) is suitable for the case that $b_p(f_1)$ is positive and $b_p(f_2)$ is negative For the case that $0 \geq b_p(f_1) > b_p(f_2)$, an inductor should be parallel connected to a serial $LC$ resonator as shown in Fig. 2(c). On the contrary, if we need $b_p(f_1) > b_p(f_2) > 0$, we need to parallel connect a capacitor with the serial $LC$ resonator, as shown in Fig. 2(d).

Based on the needed values of susceptances at two frequencies we can have two equations with two or three unknowns. For the cases of Fig. 2(a) and Fig. 2(b), the element values can be directly solved. For the other two cases, we should select the value of one element and the other two unknowns can be solved then.

As to the serial reactances, we also have four types of circuit blocks as shown in Fig. 4. We choose the suitable serial circuit blocks according to the needed values of $x_s(f_1)$ and $x_s(f_2)$.

## 3. DESIGN EXAMPLES AND DISCUSSIONS

We construct a frequency-dependent complex load which contains an inductor $L_l = 5\,\text{nH}$, a capacitor $C_l = 1\,\text{pF}$ and a resistor $R_l = 200\,\Omega$, as shown in Fig. 4.

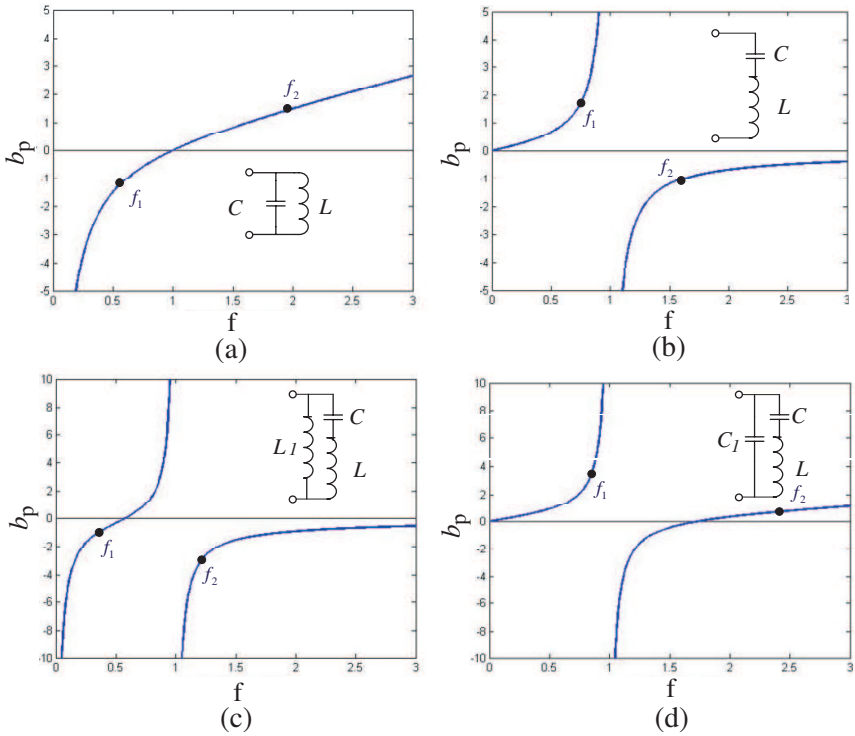


**Figure 2.** Dual-frequency susceptance circuits. (a) $b_p(f_1) < b_p(f_2)$. (b) $b_p(f_1) > 0 > b_p(f_2)$. (c) $0 \geq b_p(f_1) > b_p(f_2)$. (d) $b_p(f_1) > b_p(f_2) > 0$.

The normalized impedance of the load is given in Equation (6). Fig. 4(b) gives the plots of the real parts of the input impedance and admittance.

$$z_l(\omega) = \left(j\omega L_l + \frac{1}{1/R_l + j\omega C_l}\right) \Big/ Z_0 \tag{6}$$

Here $Z_0$ is matched impedance $50\,\Omega$.

### 3.1. Design Examples for Case A

As can be observed in Fig. 4(b), the real part of $z_l$ is below unit line within the frequency range of $1.35 \sim 4\,\text{GHz}$, meaning the complex load is outside of the $1 + jx$ circle in Smith chart. Type-I topology is suitable for dual-frequency impedance matching if $f_1$ and $f_2$ are in this frequency range. For example if $f_1 = 1.6\,\text{GHz}$ and $f_2 = 3.5\,\text{GHz}$,

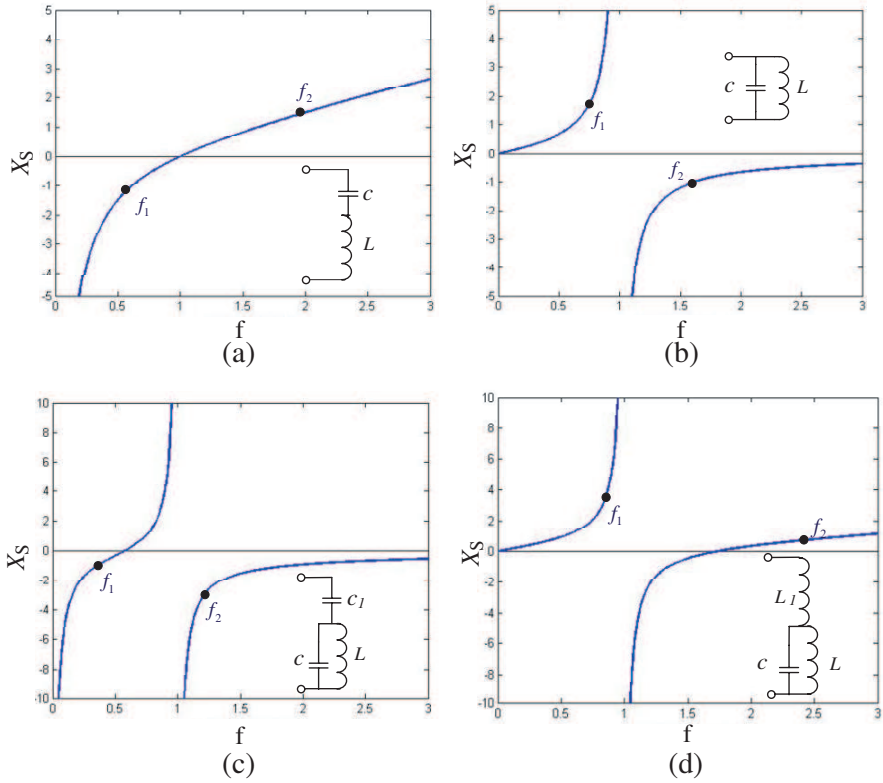


**Figure 3.** Dual-frequency reactance circuits. (a) $x_s(f_1) < x_s(f_2)$. (b) $x_s(f_1) > 0 > x_s(f_2)$. (c) $0 \geq x_s(f_1) > x_s(f_2)$. (d) $x_s(f_1) > x_s(f_2) > 0$.

we have normalized input impedances and admittances as:

$$z_l(f_1) = 0.7932 - 0.5896j;\ z_l(f_2) = 0.1966 + 1.3344j$$
$$y_l(f_1) = 0.8120 + 0.6036j;\ y_l(f_2) = 0.1081 - 0.7335j$$

*3.1.1. Step 1: $L_1$- > $A_1$ and $L_2$- > $A_2$.*

According to Equation (1) we get the reactances of the $jx_s$ block:

$$x_s(f_1) = 0.9946 \text{ or } 0.1846;\ \ x_s(f_2) = -0.9369 \text{ or } -1.7318$$

We choose: $x_s(f_1) = 0.9946;\ x_s(f_2) = -0.9369$.

*3.1.2. Step 2: $A_1$- > $O$ and $A_2$- > $O$.*

By using Equation (2) we get the sucepatances of the $jb_p$ block as:

$$b_p(f_1) = 0.5105;\ b_p(f_2) = 2.0314$$

According to Fig. 2 and Fig. 3, both the $jx_s$ block and $jb_p$ block can be realized with a parallel $LC$ circuit thus we get the circuit of the impedance transformer as shown in Fig. 5.

The values of $C_{p1}$ and $L_{p1}$ can be achieved by solving the following two equations:

$$\omega_1 C_{p1} - 1/(\omega_1 L_{p1}) = 1/(x_s(f_1) \cdot Z_0)$$
$$\omega_2 C_{p1} - 1/(\omega_2 L_{p1}) = 1/(x_s(f_2) \cdot Z_0)$$

We get: $C_{p1} = 1.7556\,\text{pF}$; $L_{p1} = 2.6345\,\text{nH}$.
Similarly we get: $C_{p2} = 2.0557\,\text{pF}$; $L_{p2} = 9.5136\,\text{nH}$.

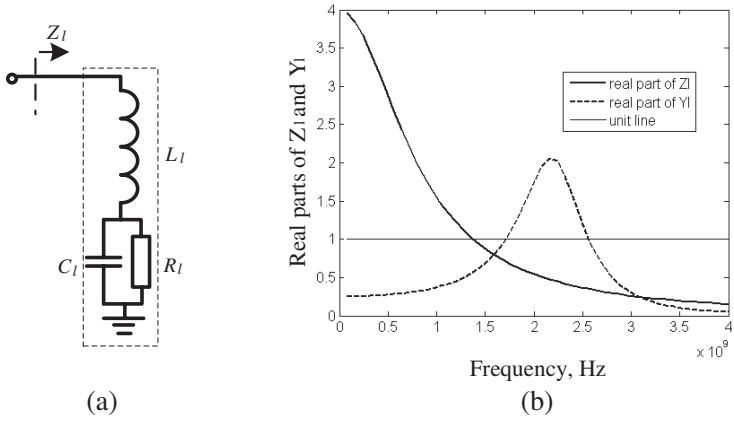


**Figure 4.** A frequency-dependent complex load. (a) Circuit. (b) Plots of the real parts of normalized input impedance and admittance

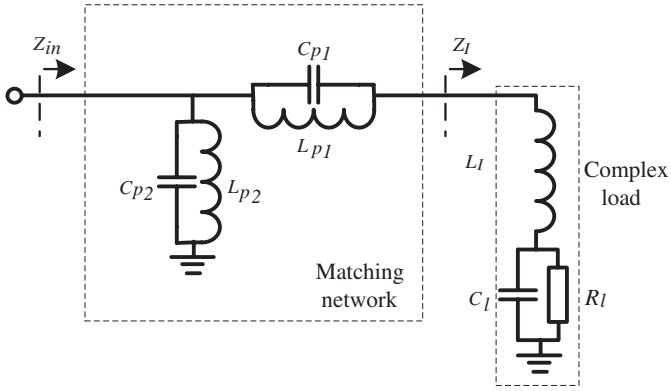


**Figure 5.** The circuit of the designed dual-frequency impedance transformers (Case A).

With the same circuit topology, we have designed two other dual-frequency transformers which have different matching frequencies and the data of all the three designs are listed in Table 1.

**Table 1.** Design data of dual-frequency impedance transformers (Case A).

| $f_1/f_2$ (GHz) | $x_s(f_1)$ | $x_s(f_2)$ | $b_p(f_1)$ | $b_p(f_2)$ |
|---|---|---|---|---|
| 1.6/3.5 | 0.9946 | −0.9369 | 0.5105 | 2.0314 |
| 1.8/3.2 | 0.8240 | −0.6511 | 0.7274 | 1.8145 |
| 2.0/3.0 | 0.6152 | −0.4534 | 0.9106 | 1.6742 |

| $C_{p1}$(pF) | $L_{p1}$(nH) | $C_{p2}$(pF) | $L_{p2}$(nH) |
|---|---|---|---|
| 1.7556 | 2.6345 | 2.0557 | 9.5136 |
| 3.2282 | 1.4547 | 2.0450 | 10.304 |
| 6.2816 | 0.7140 | 2.0382 | 10.752 |

The $s_{11}$ plots of the three impedance transformers are compared in Fig. 6. For each design, perfect matching is achieved at the specified two frequencies with 15 dB matching bandwiths of several hundreds MHzs.

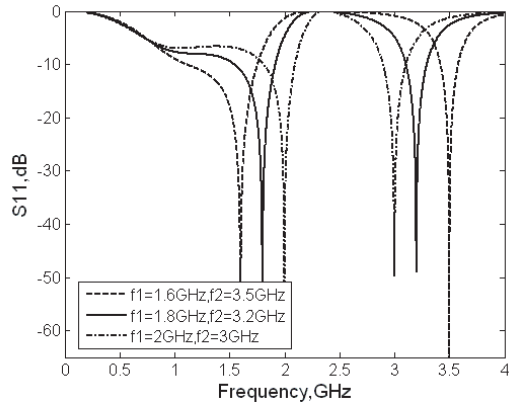


**Figure 6.** $S_{11}$ plots of designed dual-frequency impedance transformers (Case A).

### 3.2. Design Examples for Case B

The real part of normalized admittance is below unit line within the frequency range of DC-1.7 GHz, so the topology of Fig. 1(b) can be used

for dual-frequency impedance matching when $f_1$ and $f_2$ are within this range.

*3.2.1. Step 1: $L_1$- > $B_1$ and $L_2$- > $B_2$.*

If we choose $f_1 = 0.4\,\text{GHz}$ and $f_2 = 0.8\,\text{GHz}$ the susceptances of the $jb_\text{p}$ block can be achieved using Equation (3):

$$b_p(f_1) = -0.5541 \text{ or } 0.3290; \qquad b_p(f_2) = 0.2253 \text{ or } -0.7083$$

We choose $b_p(f_1) = -0.5541$ and $b_p(f_2) = 0.2253$ thus the $jb_\text{p}$ block can be realized with a parallel $LC$ circuit with the element values:

$$C_p = 2.6651\,\text{pF}; \quad L_{p1} = 22.378\,\text{nH}$$

*3.2.2. Step 2: $B_1$- > $O$ and $B_2$- > $O$.*

Then from Equation (4) we get the reactances of the $jx_s$ block at $f_1$ and $f_2$:

$$x_s(f_1) = -1.6635 \text{ and } x_s(f_2) = 1.4548$$

The $jx_s$ block can be realized with a serial $LC$ circuit whose element values are solved from the equations:

$$\omega_1 L_s - 1/(\omega_1 C_s) = x_s(f_1) \cdot Z_0$$
$$\omega_2 L_s - 1/(\omega_2 C_s) = x_s(f_2) \cdot Z_0$$

We get $C_s = 2.4963\,\text{pF}$ and $L_s = 30.326\,\text{nH}$. The circuit of the designed transformer is then shown in Fig. 7.

We list in Table 2 the data of three similar designs with different ratios between $f_1$ and $f_2$. They share the same circuit topology as shown in Fig. 7. Fig. 8 gives the compared $S_{11}$ plots of the three

**Table 2.** Design data of dual-frequency impedance transformers (Case B).

| $f_1/f_2$ (GHz) | $b_p(f_1)$ | $b_p(f_2)$ | $x_s(f_1)$ | $x_s(f_2)$ |
|---|---|---|---|---|
| 0.4/0.8 | −0.5541 | 0.2253 | −1.6635 | 1.4548 |
| 0.4/1.1 | −0.5541 | 0.1310 | −1.6635 | 1.1987 |
| 0.4/1.3 | −0.5541 | 0.0446 | −1.6635 | 0.9712 |

| $C_p$(pF) | $L_p$(nH) | $C_s$(pF) | $L_s$(nH) |
|---|---|---|---|
| 2.6651 | 22.378 | 2.4963 | 30.326 |
| 1.1089 | 28.688 | 3.2893 | 15.036 |
| 0.58183 | 31.718 | 3.6714 | 10.027 |

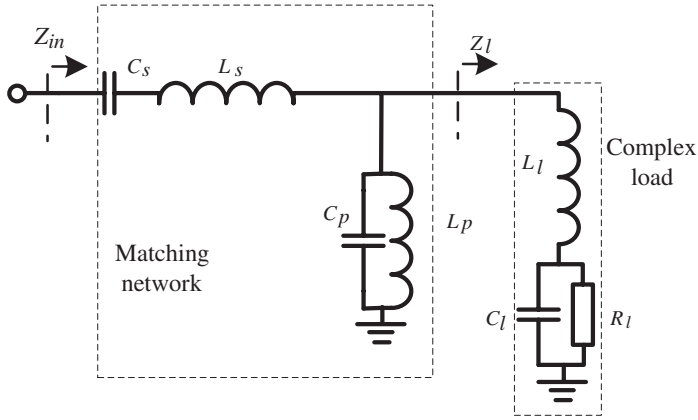


**Figure 7.** The circuit of the designed dual-frequency impedance transformers (Case B).

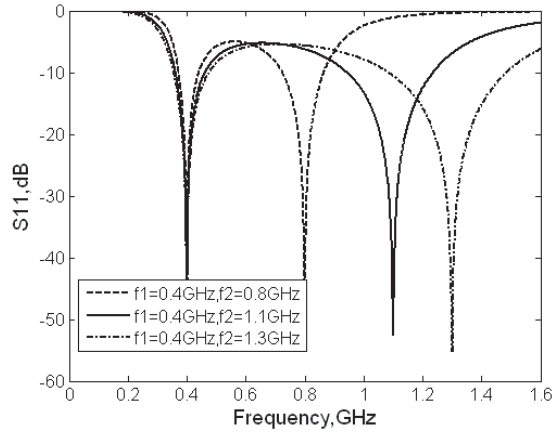


**Figure 8.** $S_{11}$ plots of designed dual-frequency impedance transformers (Case B).

examples. Big matching bandwidths are observed around the two frequencies of each example.

### 3.3. Design Examples for Case C

$z_l(f_1)$ is within the $1 + jx$ circle when $f_1$ is below 1.35 GHz while $z_l(f_2)$ is within $1 + jb$ circle when $f_2$ is within $1.7 \sim 2.6$ GHz,as can be observed in Fig. 4(b).

As an example, if we have $f_1 = 1$ GHz and $f_2 = 2$ GHz, we can list the normalized input impedances and admittances at the two

frequencies as below:

$$z_l(f_1) = 1.5509 - 1.3206j; \quad z_l(f_2) = 0.5467 - 0.1174j$$
$$y_l(f_1) = 0.3738 + 0.3183j; \quad y_l(f_2) = 1.7485 + 0.3754j$$

*3.3.1. Step 1: $L_2$ unchanged and $L_1$- > $L_1'$.*

As can be seen in the Smith chart of Fig. 9, the load impedances at $f_1$ and $f_2$ are located at $L_1$ and $L_2$ which are respectively within $1 + jx$ circle and $1 + jb$ circle. The first step is to convert case C to case A, making the impedances at the two frequencies to be outside of the $1 + jx$ circle. A shunt susceptance $jb_{p1}$ should be parallel connected to the load for this purpose and according to (5) we have:

$$b_{p1}(f_2) = 0; \quad b_{p1}(f_1) = -1.2458 \text{ or } 0.6092.$$

We choose $b_{p1}(f_1) = -1.2458$ so that the $jb_{p1}$ block can be realized using a parallel circuit of $C_{p1}$ and $L_{p1}$, which resonates on $f_2$. We have two equations:

$$j\omega_1 C_{p1} - j/(\omega_1 L_{p1}) = jb_{p1}(f_1)/Z_0 = -j0.02492$$
$$j\omega_2 C_{p1} - j/(\omega_2 L_{p1}) = jb_{p1}(f_2)Z_0 = 0$$

By solving the simultaneous equations we get:

$$C_{p1} = 1.3218\,\text{pF} \quad \text{and} \quad L_{p1} = 4.7907\,\text{nH}$$

Then we get the input impedance and admittances of $z_l'$:

$$z_l'(f_1) = 0.3738 + 0.9275j; \quad z_l'(f_2) = z_l(f_2)$$
$$y_l'(f_1) = 0.3738 - 0.9275j; \quad y_l'(f_2) = y_l(f_2)$$

The position of $z_l'(f_1)$ is $L_1'$ which is on the vertical axe. $z_l'(f_2)$ is still at the former position $L_2$.

*3.3.2. Step 2: $L_1'$- > $A_1$ and $L_2$- > $A_2$.*

In the second step $z_l'$ is connected with a serial block $jx_s$ and we get input impedance $z_A$ which is on $1+jb$ circle at both the two frequencies. According to Equation (1) we have:

$x_s(f_1) = -0.4437$ or $1.4113$ and $x_s(f_2) = 0.6152$ or $-0.3804$

We choose $x_s(f_1) = -0.4437$ and $x_s(f_2) = 0.6152$ thus the reactance block can be realized with a serial $LC$ circuit whose elements are: $L_s = 4.4412\,\text{nH}$ and $C_s = 3.1767\,\text{pF}$. By now the normalized input impedances and admittances are:

$$z_A(f_1) = 0.3738 + 0.4838j, \; y_A(f_1) = 1 - 1.2944j;$$
$$z_A(f_2) = 0.5479 + 0.4978j, \; y_A(f_2) = 1 - 0.9106j;$$

Both $z_A(f_1)$ and $z_A(f_2)$ are located on the $1 + jb$ circle.

*3.3.3. Step 3:* $A_1 -> O$ *and* $A_2 -> O$.

As a final step, a parallel $jb_p$ block is used to compensate the imaginary parts of $y_A(f_1)$ and $y_A(f_2)$, we have:

$$b_p(f_1) = -\mathrm{Im}(y_A(f_1)) = 1.2944$$
$$\text{and} \quad b_p(f_2) = -\mathrm{Im}(y_A(f_2)) = 0.9106$$

Since $b_p(f_1) > b_p(f_2) > 0$, we use a three-element circuit containing $C_e$, $C_{s1}$ and $L_{s1}$, as shown in Fig. 10 to realize the susceptance. If the serial circuit of $C_{s1}$ and $L_{s1}$ has a susceptance of $jB'_p$, we have

$$b_p(f_1)/Z_0 - \omega_1 C_e = B'_p(f_1) > 0$$
$$b_p(f_2)/Z_0 - \omega_2 C_e = B'_p(f_2) < 0$$

So: $\frac{b_p(f_1)Z_0}{\omega_1} > C_e > \frac{b_p(f_2)Z_0}{\omega_2}$

For convenience, we choose:

$$C_e = \left(\frac{b_p(f_1)Z_0}{\omega_1} + \frac{b_p(f_2)Z_0}{\omega_2}\right) \Big/ 2 = 2.7847\,\mathrm{pF}$$

And then we get the values of $C_{s1}$ and $L_{s1}$ as below:

$$C_{s1} = 0.8013\,\mathrm{pF} \quad \text{and } L_{s1} = 12.645\,\mathrm{nH}$$

From Fig. 9 we can see the matching paths for the two frequencies are: $L_1 -> L'_1 -> A_1 -> O$ and $L_2 -> A_2 -> O$. We list in Table 3 three designs including the given example. They have the same circuit topology as Fig. 10 but work on different frequencies. Fig. 11 compares the $S_{11}$ plots of the three designs and the matching bandwidths are relatively big. The biggest frequency ratio of the three designs is five. As the frequency ratio $(f_2/f_1)$ is bigger, $C_{\mathrm{p1}}$ becomes smaller and $L_{\mathrm{p1}}$ becomes bigger, meaning the circuits are becoming unrealizable.

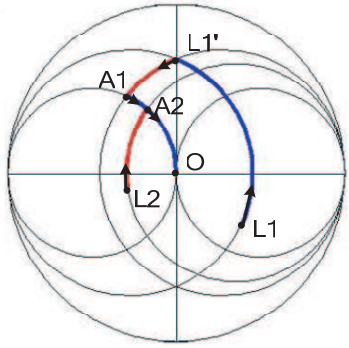


**Figure 9.** Dual-frequency impedance matching paths for a frequency-dependent complex load (Case C).

### 3.4. Discussions

The three types of design examples have demonstrated that the proposed topologies are able to achieve dual-frequency impedance matching for a variety of passive loads. The possible ratio between the matching frequencies can be big enough, ensuring enough matching bandwidths. The synthesized circuits have suitable element values that can be realized without heavy nonlinearity in microwave frequency ranges. We should note that different dual-frequency values of the $jb_p$ and $jx_s$ will incur different selection of lumped circuit blocks, thus having effect on the matching performances. Also, it can be understand that a load with smoothly-varying impedance will have bigger matching bandwidths than those with heavy fluctuations in impedances. These topologies will be suitable except the synthesized circuits have elements with unrealizable values, which happens when the load impedances or the frequency ratios ($f_2/f_1$) become extreme.

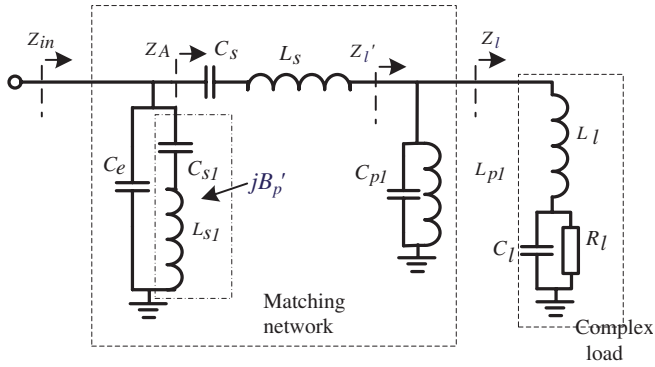


**Figure 10.** The circuit of the designed dual-frequency impedance transformers (Case C).

**Table 3.** Design data of dual-frequency impedance transformers (Case C).

| $f_1/f_2$(GHz) | $b_{p1}(f_1)$ | $b_{p1}(f_2)$ | $C_{p1}$(pF) | $L_{p1}$(nH) | $x_s(f_1)$ | $x_s(f_2)$ | $C_s$(pF) | $L_s$(nH) |
|---|---|---|---|---|---|---|---|---|
| 1.0/2.0 | −1.2458 | 0 | 1.3218 | 4.7907 | −0.4437 | 0.6152 | 3.1767 | 4.4412 |
| 0.7/2.3 | −1.1600 | 0 | 0.53849 | 8.8921 | −0.4942 | 0.2856 | 7.0998 | 1.6626 |
| 0.5/2.5 | −1.1040 | 0 | 0.29286 | 13.839 | −0.5151 | 0.0676 | 11.561 | 0.56564 |
| $f_1/f_2$ (GHz) | $b_p(f_1)$ | $b_p(f_2)$ | $C_e$(pF) | $L_{s1}$(nH) | $C_{s1}$(pF) | | | |
| 1.0/2.0 | 1.2944 | 0.9106 | 2.7847 | 12.645 | 0.8013 | | | |
| 0.7/2.3 | 1.5205 | 1.1569 | 4.2577 | 3.9729 | 2.2062 | | | |
| 0.5/2.5 | 1.6247 | 1.3105 | 6.0058 | 1.9467 | 4.0036 | | | |

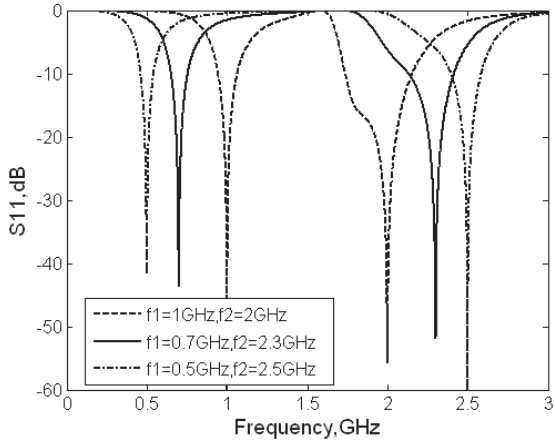


**Figure 11.** $S_{11}$ plots of designed dual-frequency impedance transformers (Case C).

## 4. CONCLUSIONS

Three types of circuit topologies are proposed for dual-frequency impedance matching for arbitrary frequency-dependent complex loads by extending the impedance matching concepts of L-type networks. Impedance matching processes are described on Smith chart with design formula deduced. For realizing the needed dual-frequency susceptances and reactances, different lumped circuit blocks are adopted. A variety of design examples are given and compared validating the feasibility of the method. Big frequency ratios and bandwidths are achieved. These dual-frequency transformers use limited number of lumped elements and will afford much compacter dimension compared to other distributive alternatives.

## ACKNOWLEDGMENT

The work was supported by NUAA Research Funding, No. NS2010105. It was also supported in part by the Open Research Program of State Key Laboratory of Millimeter Waves under Grant K201221.

## REFERENCES

1. Anguera, J., C. Puente, and C. Borja, "Dual frequency broadband microstrip antenna with a reactive loading and stacked elements," *Progress In Electromagnetics Research Letters*, Vol. 10, 1–10, 2009.

2. Behera, S. and K. J. Vinoy, "Microstrip square ring antenna for dual-band operation," *Progress In Electromagnetics Research*, Vol. 93, 41–56, 2009.
3. Alkanhal, M. A. S., "Dual-band bandpass-fillters using inverted stepped-impedance resonators," *Journal of Electromagnetic Waves and Applications*, Vol. 23, Nos. 8–9, 1211–1220, 2009.
4. Fallahzadeh, S., H. Bahrami, and M. Tayarani, "A novel dual-band bandstop waveguide filter using split ring resonators," *Progress In Electromagnetics Research Letters*, Vol. 12, 133–139, 2009.
5. Lin, W.-J., C.-S. Chang, J.-Y. Li, D.-B. Lin, L.-S. Chen, and M.-P. Houng, "A new approach of dual-band filters by stepped impedance simplified cascaded quadruplet resonators with slot coupling," *Progress In Electromagnetics Research Letters*, Vol. 9, 19–28, 2009.
6. Velazquez-Ahumada, M. D. C., J. Martel-Villagr, F. Medina, and F. Mesa, "Application of stub loaded folded stepped impedance resonators to dual band filters," *Progress In Electromagnetics Research*, Vol. 102, 107–124, 2010.
7. He, J., B.-Z. Wang, and K.-H. Zhang, "Arbitrary dual-band coupler using accurate model of composite right/left handed transmission line," *Journal of Electromagnetic Waves and Applications*, Vol. 22, Nos. 8–9, 1267–1272, 2008.
8. De Castro-Galan, D., L. E. Garcia Munoz, D. Segovia-Vargas, and V. Gonzalez-Posadas, "Diversity monopulse antenna based on a dual-frequency and dual mode CRLH rat-race coupler," *Progress In Electromagnetics Research B*, Vol. 14, 87–106, 2009.
9. Lin, Z. and Q.-X. Chu, "A novel approach to the design of dual-band power divider with variable power dividing ratio based on coupled-lines," *Progress In Electromagnetics Research*, Vol. 103, 271–284, 2010.
10. Chaudhary, G., Y. Jeong, K. Kim, and D. Ahn, "Design of dual-band bandpass filters with controllable bandwidths using new mapping function," *Progress In Electromagnetics Research*, Vol. 124, 17–34, 2012.
11. Chen, W.-Y., M.-H. Weng, S.-J. Chang, H. Kuan, and Y.-H. Su, "A new tri-band bandpass filter for GSM, WiMAX and ultra-wideband responses by using asymmetric stepped impedance resonators," *Progress In Electromagnetics Research*, Vol. 124, 365–381, 2012.
12. Liu, J.-C., K.-D. Yeh, C.-C. Yen, C.-Y. Liu, B.-H. Zeng, and C.-C. Chen, "Miniaturized dual-mode resonators with improved

double square loop and inter-digital couple for WLAN dual-bands," *Progress In Electromagnetics Research C*, Vol. 24, 123–136, 2011.

13. Shao, J., H. Zhang, C. Chen, S. Tan, and K. J. Chen, "A compact dual-band coupled-line balun with tapped open-ended stubs," *Progress In Electromagnetics Research C*, Vol. 22, 109–122, 2011.
14. Wang, C.-J., Y.-J. Lee, and K.-C. Lee, "A dual-band CPW-FED l-slot antenna with both linear and circular polarizations," *Progress In Electromagnetics Research C*, Vol. 21, 229–241, 2011.
15. Li, X., Y.-J. Yang, L. Yang, S.-X. Gong, X. Tao, Y. Gao, K. Ma, and X.-L. Liu, "A novel design of dual-band unequal wilkinson power divider," *Progress In Electromagnetics Research C*, Vol. 12, 93–100, 2010.
16. Li, W.-M., Y.-C. Jiao, L. Zhou, and T. Ni, "Compact dual-band circuilarly polarized monopole antenna," *Journal of Electromagnetic Waves and Applications*, Vol. 25, No. 14–15, 2130–2137, 2011.
17. Monzon, C., "A small dual-frequency transformer in two sections," *IEEE Transactions on Microwave Theory and Techniques*, Vol. 51, No. 4, 1157–1161, 2003.
18. Park, M. J. and B. Lee, "Dual band design of single stub impedance matching networks with application to dual band stubbed T junctions," *Microw. Opt. Technol. Lett.*, Vol. 52, No. 6, 1359–1362, 2010.
19. Wu, Y., Y. Liu, and S. Li, "A dual-frequency transformer for complex impedances with two unequal sections," *IEEE Microw. Wirel. Compon. Lett.*, Vol. 19, No. 2, 77–79, 2009.
20. Liu, X., Y. Liu, S. Li, F. Wu, and Y. Wu, "A three-section dual-band transformer for frequencydependent complex load impedance," *IEEE Microw. Wirel. Compon. Lett.*, Vol. 19, No. 10, 611–613, 2009.
21. Chuang, M. L., "Dual-band impedance transformer using two-section shunt stubs," *IEEE Transactions on Microwave Theory and Techniques*, Vol. 58, No. 5, 1257–1263, 2010.
22. Nikravan, M. A. and Z. Atlasbaf, "T-section dual-band impedance transformer for frequency-dependent complex impedance loads," *Electronics Letters*, Vol. 47, No. 9, 551–553, Apr. 2011.
23. Wu, Y., Y. Liu, S. Li, C. Yu, and X. Liu, "A generalized dual-frequency transformer for two arbitrary complex frequency-dependent impedances," *IEEE Microw. Wirel. Compon. Lett.*, Vol. 19, No. 12, 792–794, 2009.

24. Fukuda, A., H. Okazaki, and S. Narahashi, "Novel multi-band matching scheme for highly efficient power amplifier," *Proceedings of the 39th European Microwave Conference*, 1086–1089, Rome, Italy, Sep. 2009.
25. Nallam, N. and S. Chatterjee, "Design of concurrent multi-band matching networks," *IEEE International Symposium on Circuits and Systems*, 201–204, Rio de Janeiro, Brazil, May 2011.